

Table 3 (cont.)

<i>hkl</i>	$F_{obs.}$	$F_{calc.}$	<i>hkl</i>	$F_{obs.}$	$F_{calc.}$	<i>hkl</i>	$F_{obs.}$	$F_{calc.}$
025	13	-15	12.0.1	6	+8	503	5	+9
035	<4	-0	13.0.1	21	-19	603	6	-3
045	<4	+7	14.0.1	<4	+0	703	16	-15
055	<4	+4				803	7	+8
			102	7	+4	903	<4	-5
006	4	-4	202	49	+48			
016	<3	+1	302	20	+15	104	7	-5
026	<3	-1	402	40	+36	204	<4	+5
036	7	-10	502	30	-30	304	6	-9
046	<3	+1	602	15	+11	404	6	+3
			702	<3	-1	504	12	+12
101	5	+8	802	<4	-2	604	<4	+7
201	51	+60	902	20	-24	704	7	+3
301	39	-36	10.0.2	10	-9			
401	40	-32	11.0.2	<4	-3	105	<4	+3
501	<3	-0	12.0.2	<4	-1	205	5	+5
601	12	+8	13.0.2	6	+5	305	11	-9
701	<3	+4				405	<4	-0
801	9	-8	103	20	-19	505	<4	-5
901	13	-8	203	29	-33			
10.0.1	<4	-1	303	11	+9	106	4	+8
11.0.1	8	-7	403	14	-12	206	<3	+0

*Acta Cryst.* (1950). **3**, 333

## The Covalent Bond in Diamond and the X-ray Scattering Factor of Covalent-Bonded Carbon

BY R. BRILL\*

*Signal Corps Engineering Laboratories, Fort Monmouth, New Jersey, U.S.A.*

(Received 6 December 1949)

By Fourier synthesis it was found that the change which a carbon atom undergoes forming a covalent bond consists in concentrating about one-half to three-quarters of one electron of the outer shell in every chemical bond. An X-ray atomic scattering curve is given for the covalent-bonded carbon atom.

Precision measurements of the X-ray diffraction patterns of diamond show appreciable deviations from the theoretical values for the atomic scattering power of carbon as given by both Hartree and Pauling (Brill, Grimm, Hermann & Peters, 1939). Fig. 1 shows the Hartree (*H*) and Pauling (*P*) scattering curves and the measured values. These deviations may be caused by lack of spherical symmetry of the carbon atom in the diamond lattice or by the inaccuracy of the theoretical curves even for the spherical atom.

Because the knowledge of the scattering curve for the carbon atom is important for the determination of atomic arrangements in organic compounds, it seemed worth while to investigate the significance of the differences between the experimental and the theoretical values. This was tried by means of a two-dimensional Fourier synthesis of the projection on the 110 plane of the diamond lattice, using these differences as amplitudes according to

$$\begin{aligned} \Delta\rho(x, z) &= \rho(x, z)_{\text{exp.}} - \rho(x, z)_{\text{theor.}} \\ &= \frac{1}{f} \sum_h \sum_l \Delta F_{h0l} \exp [2\pi i(xh + zl)]. \end{aligned}$$

\* Present address: Polytechnic Institute of Brooklyn, Brooklyn, N.Y., U.S.A.

The indices in this formula are referred to a tetragonal cell with  $a_1 = a\sqrt{2}$  and  $c_1 = a$ , where  $a$  means the length of the cubic elementary cell of diamond. (The indices

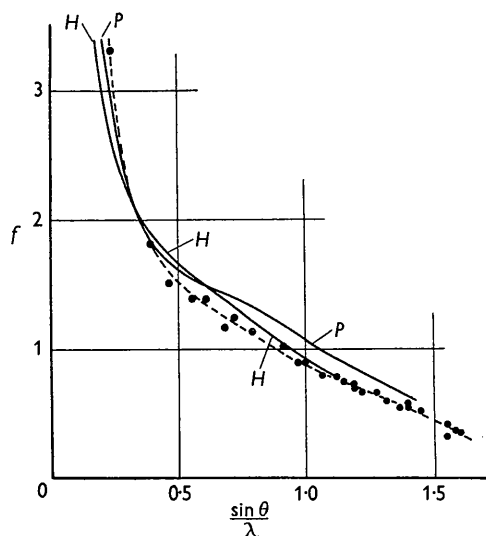


Fig. 1. Comparison of measured atomic scattering factors (dots) and the Hartree (*H*) and Pauling (*P*) scattering curves.

given in the table are referred to the normal cubic diamond cell.)  $\Delta F_{h0l}$  denotes the difference

$$F_{h0l, \text{exp.}} - F_{h0l, \text{theor.}}$$

The value  $\Delta\rho$  gives obviously the change of electron density which we obtain if we replace a centro-symmetrical carbon atom by the carbon atom in diamond with its strong covalent bonds in the tetrahedral directions. Where  $\Delta\rho$  is positive we find an excess, and where it is negative a deficiency compared with that density which would result from centrosymmetric atoms.

Fig. 1 shows that at high  $(\sin \theta)/\lambda$  values the Hartree curve approximates closely to the experimental curve. Therefore, the assumption was made that all reflexions with  $(\sin \theta)/\lambda > 1.1$  agree with the theoretical Hartree curve. This assumption appears reasonable in view of the fact that the inner parts of the electron cloud of the atom are not influenced much by the chemical bond.

Table 1 shows the values used for the calculations.

Fig. 1 shows that the same procedure cannot be applied if the calculation is based on the Pauling curve. In this case the deviations at higher angles are large. Therefore, the Pauling curve was extrapolated to  $(\sin \theta)/\lambda = 1.65$  and an artificial temperature factor of the form  $\exp[-0.023 \sum_i h_i^2]$  was applied, this having the

effect of making the smallest amplitude approximately 3% of the largest one. Obviously this procedure is not

Table 1.  $F$  values used for calculations according to the Hartree model

Indices	$F_{\text{theor.}}$	$F_{\text{exp.}}$	$F_{\text{exp.}} - F_{\text{theor.}} = \Delta F$
111	-1.810	-2.333	-0.52
022	1.87	1.805	-0.07
311	1.21	1.060	-0.15
222	0.0	0.138	0.14
400	-1.57	-1.381	0.19
133	-1.06	-0.972	0.09
422	-1.39	-1.166	0.22
333	0.933	0.835	-0.10
511		0.850	-0.08
044	1.22	1.120	-0.10
533	0.715	0.715	0.00
444	-0.93	-0.891	0.04
155	-0.629	-0.640	-0.01
711		-0.637	-0.01
355	0.572	0.558	-0.01
800	0.77	0.776	0.01

very good, but the Pauling curve is not supposed to be as accurate as the curve given by Hartree, who used the method of self-consistent field (see, for example, Ewald, 1933, pp. 322-3). Hence this procedure may be justified; anyway, more weight will be put on the result of the calculations based on the Hartree curve. The values used for the calculations based on the Pauling curve are given in Table 2.

#### Discussion of the results

Fig. 2 shows the diamond structure in the direction of the projection, and the result of the calculations is

Table 2.  $F$  values used for calculations according to the Pauling model

Indices	$F_{\text{theor.}}$	$F_{\text{exp.}}$	$F_{\text{theor.}} - F_{\text{exp.}}$	$\Delta F \exp[-0.023 \sum_i h_i^2]$
111	-2.150	-2.333	-0.183	-0.17
022	1.84	1.805	-0.035	-0.03
311	1.81	1.060	-0.121	-0.095
222	0.0	0.138	0.138	0.105
400	-1.54	-1.381	0.159	0.11
133	-1.06	-0.972	0.088	-0.055
422	-1.44	-1.166	0.274	0.16
333	0.990	0.835	-0.155	-0.085
511	0.990	0.850	-0.140	-0.075
044	1.34	1.120	-0.220	-0.11
533	0.834	0.715	-0.119	-0.045
444	-1.11	-0.891	0.219	0.075
711	-0.757	-0.637	0.120	0.035
155	-0.757	-0.637	0.117	0.035
355	0.700	0.558	-0.142	-0.035
800	0.930	0.776	-0.154	-0.04
733	-0.636	-0.525	0.111	0.025
822	0.85	0.698	-0.152	-0.03
066	0.85	0.716	-0.134	-0.03
555	0.58	0.470	-0.110	-0.02
911	-0.537	-0.459	0.078	0.01
466	-0.72	-0.594	0.126	0.015
844	0.66	0.533	-0.127	-0.015
933	-0.453	-0.406	0.047	0.005
177	-0.453	-0.401	0.052	0.005
755	-0.453	-0.406	0.047	0.005
377	0.424	0.364	-0.060	-0.005
577	0.368	0.217	-0.151	-0.010
11.1.1	(0.368)	0.290	-0.078	-0.01
088	(0.49)	0.359	-0.131	-0.005
955	(0.34)	-0.240	0.100	0.005
866	(0.46)	0.299	-0.161	-0.005
11.3.3	(0.32)	0.147	-0.173	-0.005

given in Figs. 3 and 4. Regions with negative  $\Delta\rho$  values are shaded in Figs. 3 and 4. Both figures show some small, nearly spherical regions of negative values. As may be seen by comparison with Fig. 2, these regions obviously are the centers of the carbon atoms. They form a hexagon-like arrangement surrounding large holes in the lattice. In the regions of these holes deficiency of electron density is also found. On lines connecting two neighbor atoms we find excess.

It is evident that only regions which are farther apart from the centers of the atoms contribute to the big hole in the center of the hexagon. We may conclude from this fact that in regions far from the center of an atom the influence of the chemical bond consists in producing a deficiency by shifting electrons towards the center of an atom.

At the centers of the atoms a value of  $\Delta\rho$  equal to zero might be expected because the electrons are bound there by such strong forces that they should not be influenced by the chemical bond. Instead, in Figs. 3 and 4 negative values are found at the center. This is

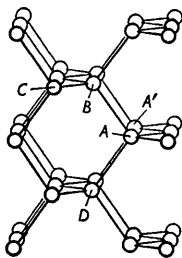


Fig. 2. Diamond structure, seen in the direction of projection.

most likely due to the fact that, *in the projection*, regions far from the center of the atoms will contribute to the projection at the center of an atom; thus, a line connecting the atoms  $A$  and  $A'$  corresponds to the line connecting  $D$  and  $B$  (Fig. 2). The deficiencies along  $BD$  project in Figs. 3 and 4 on to the atomic centres. This does not prove that negative values occur along a line  $BD$  in a three-dimensional analysis, but it makes it probable. The electron distribution from which the Hartree curve is derived may yet be correct in regions close to the center of the atom, but it is not possible to explain in the same way the negative values in Fig. 4 which is based on the Pauling model. Here the negative values in the center of the atoms are much lower than the lowest values in the big hole. Therefore, if we consider that the big hole has approximately a cylindrical symmetry, we can conclude that the electron distribution on which the Pauling scattering factor is based has too high an electron density near the center of the atom. (This is expressed also by the large deviation of the Pauling scattering curve in Fig. 1 from the experimental values at large angles.)

Along the direction of a chemical bond we find positive values of  $\Delta\rho$ , but the values between the atoms  $A$  and  $B$  are much lower than between  $C$  and  $B$  (see

Figs. 2, 3 and 4), even if we consider the fact that the line connecting  $AB$  is parallel to the plane of projection and the line connecting  $CB$  is inclined, so that overlapping

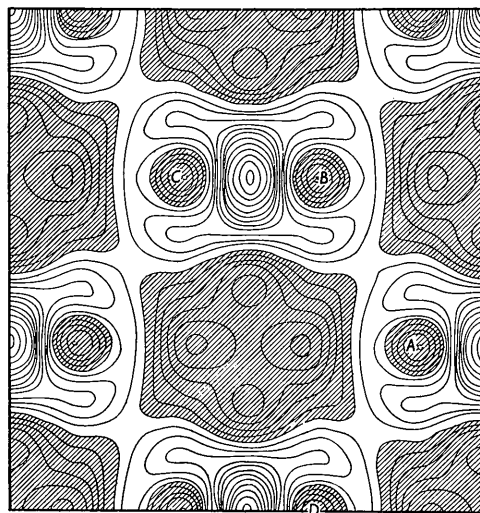


Fig. 3. Shift of electron density relative to the Hartree spherical electron distribution. Negative regions are shaded. The contour surrounding each shaded region corresponds to  $\Delta\rho=0$ . The contours in the negative regions correspond to  $-0.18, -0.36, -0.54, -0.71$  and  $-0.89$ . Those in the positive regions correspond to  $0.18, 0.36, 0.54, 0.71, 0.89, 1.07, 1.25, 1.43, 1.61, 1.79, 1.97$  and  $2.15$ . Letters correspond to the atoms in Fig. 2.

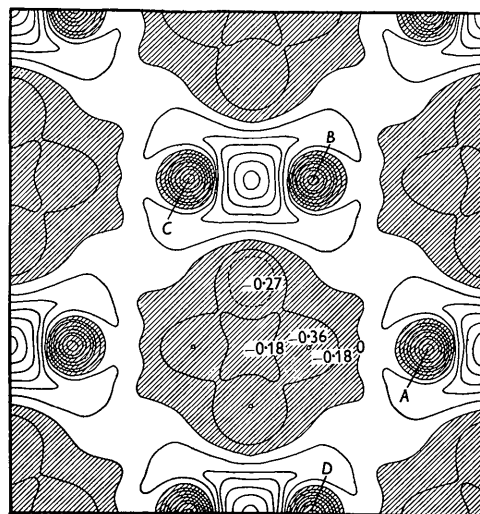


Fig. 4. Shift of electron density relative to the Pauling spherical electron distribution. Negative regions are shaded. The contour surrounding each shaded region corresponds to  $\Delta\rho=0$ . The contours in one negative region are marked; in the other negative regions they correspond to  $-0.18, -0.36, -0.54, -0.71, -0.89, -1.05$  and  $-1.25$ . The contours in the positive regions correspond to  $0.18, 0.36, 0.54, 0.71, 0.89$  and  $1.07$ . Letters correspond to the atoms in Fig. 2.

takes place here, and that two bonds are projected on top of each other along  $CB$ . The reason for this fact is obviously that negative values from regions far from the center of an atom are also projected on the line  $AB$ . The same is the case for the area between atoms  $B$  and  $C$  but

the influence of negative values must be smaller in this case. This can easily be seen from Fig. 2 if one considers that the same projection as in Fig. 3 or 4 results in a plane which is perpendicular to the plane of the projection of Fig. 3 and contains the atoms  $A$ ,  $A'$  and  $B$ . Hence the difference of the  $\Delta\rho$  values between atoms  $A$  and  $B$  and atoms  $B$  and  $C$  can well be explained. So it can be stated qualitatively that the projections clearly show the influence of the chemical bond type to consist in an electron shift towards the line of the chemical bond, which produces the tetrahedral deformation of the electron cloud of the carbon atoms.

The other question is whether or not this two-dimensional projection permits us to find the number of electrons which are shifted into the bond direction. We will try to answer this question in two different ways on the basis of Fig. 3.

(1) Assume that the area between atoms of the kind  $B$  and  $C$  is not influenced very much by overlapping with negative values. Then an integration over a reasonable area between these atoms yields an excess value of about 0.4 electron per bond and this value should be somewhat too small.

(2) Integrate over the  $\Delta\rho$  values of a small area along a line between atoms of the kind  $B$  and  $C$  and also along a line connecting  $A$  and  $B$ , on the assumption that the negative area in the center of the atom has the value zero in reality. Then half the value obtained between  $B$  and  $C$  should be equal to the value calculated for the line  $AB$ . But half the value obtained between  $B$  and  $C$  is nearly double the value between  $A$  and  $B$ . From this fact one may conclude that the influence of overlapping by negative values along  $AB$  is nearly as great as the positive values found on this line, and this gives an estimate of the amount of deficiency projected on the bond between  $A$  and  $B$ . If one assumes that this deficiency area has a reasonable width, one obtains by integration a total electron deficiency of 0.8 electron per bond, corresponding to this area. This value must be regarded as an upper limit, considering that an integrated deficiency in the entire hexagon corresponds to 0.96 electron. On the other hand, the area of the hexagon delivers to every bond a contribution of one-quarter of an electron. Thus one obtains from the negative areas a total shift of one electron per bond.

Considering that method (2) is very rough and that estimation (1) gives a value which is certainly too small, we are able to conclude that, relative to the Hartree distribution of a spherical atom, one-half to three-quarters of an electron has been shifted into each bond in a first approximation.

Now Fig. 1 shows that the 111 reflexion differs very much from the theoretical value given by Hartree and it may be worthwhile further to discuss this difference. The experimental value, given by Brill *et al.* (1939), is  $F_{111} = 2.333$ . This value was measured on a very fine diamond powder and is supposed to be uninfluenced by extinction. The difference, therefore, should be real.

To see how this large deviation of the intensity of the 111 reflexion influences the result of Fig. 3, the contribution of  $\Delta F_{111}$  was subtracted from the projection of Fig. 3, leading to Fig. 5. Fig. 5 looks less reasonable than Fig. 3 because the background is less smooth and, especially, because the negative areas at the centers of the atoms are larger and much deeper. The experimental value for  $F_{111}$ , therefore, seems to be reasonable, and a higher average value of the atomic scattering factor must be assumed at low angles for atoms with four covalent bonds in the tetrahedral directions. This means that the atomic scattering factor is given better at low angles by the Pauling curve and at higher angles by the Hartree curve.

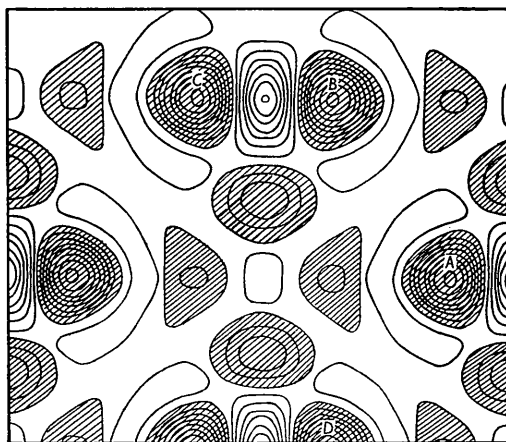


Fig. 5. Same projection as Fig. 3 but without contribution of 111. Negative regions are shaded. The contour surrounding each shaded region corresponds to  $\Delta\rho = 0$ . The contours in the negative regions correspond to  $-0.18$ ,  $-0.36$ ,  $-0.54$ ,  $-0.71$ ,  $-0.89$ ,  $-1.05$  and  $-1.25$ . Those in the positive regions correspond to  $0.18$ ,  $0.36$ ,  $0.54$ ,  $0.71$ ,  $0.89$ ,  $1.05$  and  $1.25$ . Letters correspond to the atoms in Fig. 2.

It may therefore be better to use the values given by the broken line in Fig. 1 for the atomic scattering factor of carbon in compounds with covalent single-bond type, even though the scattering factor of an atom without spherical symmetry cannot be described by a smooth

Table 3. Atomic scattering factor for a tetrahedral covalent-bonded carbon atom at  $0^\circ$  K.

$(\sin \theta)/\lambda$	$f$
0.25	3.35
0.3	2.45
0.4	1.88
0.5	1.59
0.6	1.46
0.7	1.36
0.8	1.27
0.9	1.18
1.0	1.09
1.1	1.02
1.2	0.97
1.3	0.91
1.4	0.82
1.5	0.75
1.6	0.62

curve on a plane, since the deviations of the experimental values from the smooth curve are obviously smaller than from either the Hartree or the Pauling curve.

The curves of Fig. 1 correspond to  $f$  values at room temperature for the diamond lattice. From these the values for 0° K. shown in Table 3 are calculated.

The calculations were carried out by means of I.B.M. machines, using a punched-card file which Prof. Schomaker, Pasadena, kindly prepared. I am

very much obliged to Mr I. A. Poole for his kind help in wiring the plug-board of the I.B.M. Tabulator and in operating the I.B.M. machines. Furthermore, I wish to thank Miss Hathaway, Mrs Mimi Mark and Mr B. F. Brown for the preparation of the figures.

#### References

- BRILL, R., GRIMM, H. G., HERMANN, C. & PETERS, C. (1939). *Ann. Phys., Lpz.*, (5), **34**, 393.  
 EWALD, P. P. (1933). *Handbuch der Physik*, 2nd ed., **23** (ii).

*Acta Cryst.* (1950). **3**, 337

## X-ray Diffraction Study of Cerous Phosphate and Related Crystals. I. Hexagonal Modification

BY ROSE C. L. MOONEY

*Newcomb College, Tulane University, New Orleans, La., U.S.A.*

(Received 28 November 1949)

The phosphates of trivalent lanthanum, cerium, and neodymium have been found to be dimorphic. One phase is monoclinic, isomorphous with the mineral monazite; the other is a hexagonal structure of a new type which easily converts to the monoclinic form at moderately high temperatures.

The hexagonal modification crystallizes with the symmetry of  $D_6^4-C_6^2$ . There are three molecules of  $XPO_4$  in the unit hexagonal cell, where  $X$  may be La, Ce or Nd. The cell dimensions of the three crystals have been determined, and the complete structure has been deduced. In this structure  $X$  is co-ordinated to eight oxygen atoms—four at 2.34 Å. and four at 2.66 Å.—in such a manner as to leave open, oxygen-lined channels along the hexagonal axis. The presence of zeolitic water in these channels [ $XPO_4(0-0.5H_2O)$ ] is probably necessary to stabilize the structure.

### Introduction

This investigation of the crystalline structure of the phosphates of lanthanum, cerium (ous), praseodymium and neodymium was carried out at the Metallurgical Laboratory of the University of Chicago in 1944. A brief résumé of the results has appeared in a letter to the Editor of the *Journal of Chemical Physics* (Mooney, 1948). The compounds were prepared in the form of powder precipitates from aqueous solution by members of a group of the Chemistry Division, Metallurgical Laboratory, under the direction of Dr William Rubinson. The large number of samples made under carefully controlled conditions by this group was indispensable to the successful issue of the X-ray investigation.

### The dimorphic forms

The phosphates of lanthanum and the rare earths must be expected to be isomorphous with the mineral monazite,  $(La, Ce, Di)PO_4$ , a monoclinic crystal for which the cell size and space group are reported in the literature (Parrish, 1939).

However, X-ray examination of laboratory prepared samples showed that the compounds are dimorphic, and that the two forms often coexist. The

more stable form is indeed monoclinic and isomorphous with monazite; the other is a hexagonal structure of a new type. It appears that, at moderate temperatures, the phosphates of cerium and its isomorphs usually crystallize from solution in the hexagonal form; and that they convert rapidly to the monoclinic arrangement at high temperatures. Long digestion periods in the mother liquor also tend to cause conversion to the monoclinic form. However, dried powders of the hexagonal structure type seem to be quite stable at room temperatures, and no evidence of spontaneous conversion to the more stable monoclinic type has been observed. A number of the original samples, re-examined by X-rays after a storage period of four years, were found to have retained the hexagonal structure.

The structure determination of the hexagonal crystal is discussed in the following sections. A report on the monoclinic crystal is in preparation.

### X-ray diffraction data

The diffraction photographs were taken from thin cylindrical powder samples, exposed in 9 cm. and in 18 cm. diameter Bradley-type cameras. The radiation